Mon. Not. R. Astron. Soc. **303,** 30–38 (1999)

Grids of white dwarf evolutionary models with masses from $M = 0.1$ to $1.2\,M_{\odot}$

O. G. Benvenuto★† and L. G. Althaus★‡

Facultad de Ciencias Astronómicas y Geofísicas, Universidad Nacional de la Plata, Paseo del Bosque S/N, (1900) La Plata, Argentina

Accepted 1998 October 5. Received 1998 October 5; in original form 1998 April 15

ABSTRACT

We present detailed evolutionary calculations for carbon–oxygen- and helium-core white dwarf models with masses ranging from $M = 0.1$ to $1.2\,M_{\odot}$ and for metallicities $Z = 0.001$ and 0. The sequences cover a wide range of hydrogen envelopes as well. We have taken finite-temperature effects fully into account by means of a detailed white dwarf evolutionary code, in which updated radiative opacities and equations of state for hydrogen and helium plasmas are considered. The energy transport by convection is treated within the formalism of the full-spectrum turbulence theory, as given by the self-consistent model of Canuto, Goldman & Mazzitelli. Convective mixing, crystallization, hydrogen burning and neutrino energy losses are taken into account as well.

The set of models presented here is very detailed and should be valuable, particularly for the interpretation of observational data on low-mass white dwarfs recently discovered in numerous binary configurations, and also for the general problem of determining the theoretical luminosity function for white dwarfs. In this context, we compare our cooling sequences with the observed white dwarf luminosity function recently improved by Leggett, Ruiz & Bergeron and we obtain an age for the Galactic disc of ≈ 8 Gyr. Finally, we apply the results of this paper to derive stellar masses of a sample of low-mass white dwarfs.

Key words: stars: evolution – stars: interiors – stars: luminosity function, mass function – pulsars: general – white dwarfs.

1 INTRODUCTION

Numerous observations carried out over recent years have presented strong evidence that low-mass, helium white dwarf stars are the product of the evolution of certain close binary systems. Indeed, low-mass white dwarfs have been detected in binary systems containing, for instance, another white dwarf (Marsh 1995; Marsh, Dhillon & Duck 1995; Marsh & Duck 1996; Moran, Marsh & Bragaglia 1997), a millisecond pulsar (Lundgren et al. 1996; see also Backer 1998) or a yellow giant (Landsman et al. 1997). In particular, Moran et al. (1997) found the binary system WD 0957 – 666 (consisting of two low-mass white dwarfs) to have an orbital period of only 1.46 h, which is short enough for the binary to merge within only 2.0×10^8 yr. Very recently, Edmonds et al. (1998) have reported the presence of a candidate helium white dwarf in the globular cluster NGC 6397. On theoretical grounds, recent population models of close binaries (Iben, Tutukov & Yungelson 1997) suggest a high probability of discovering helium white dwarfs in close binaries.

Detailed evolutionary models of low-mass white dwarfs may provide valuable information not only on the white dwarf itself but also on the companion object and even on the past evolution of the system (see, for instance, Burderi, King & Wynn 1996 and Hansen & Phinney 1998b). In this regard, the analysis carried out, notably by van Kerkwijk, Bergeron & Kulkarni (1996), is worth mentioning. Indeed, from spectroscopic data inferred from its low-mass white dwarf companion, combined with a theoretical mass–radius relation for the white dwarf, these authors found the mass of the pulsar PSR J1012+5307 to be between 1.5 and 3.2 $M_{\odot}$. Needless to say, detailed models of helium white dwarfs, together with further observations, are needed in order to achieve a more precise determination of the pulsar mass and hence to constrain the equation of state at the high densities appropriate for neutron stars. In addition, an independent determination of the age of many millisecond pulsars can be inferred from the study of the cooling of their helium white dwarf companions, which is valuable for understanding the nature and origin of such systems. Another strong motivation for constructing improved white dwarf evolutionary sequences is the fact that, thanks to the *Hubble Space*

†Member of the Carrera del Investigador Científico, Comision de Investigaciones Científicas de la Provincia de Buenos Aires (CIC), Argentina.
★E-mail: obenvenuto@fcaglp.fcaglp.unlp.edu.ar (OGB); althaus@fcaglp.fcaglp.unlp.edu.ar (LGA)
‡Fellow of the Consejo Nacional de Investigaciones Científicas y Técnicas (CONICET), Argentina.

Telescope, it has been possible to detect the low-luminosity tail of the white dwarf population in globular clusters. Accordingly, white dwarf evolutionary tracks would provide an independent way of measuring the age and distance of such clusters (see e.g. Richer et al. 1995; Von Hippel, Gilmore & Jones 1995; Renzini et al. 1996).

In view of these considerations, we present in this paper new grids of white dwarf evolutionary models for different hydrogen envelopes and stellar masses. The emphasis is placed mainly on low-mass, helium white dwarfs, the detailed study of which has recently began to be undertaken. As a matter of fact, Althaus & Benvenuto (1997a) and Benvenuto & Althaus (1998) carried out an analysis of the structure and evolution of low-mass white dwarfs based on a updated physical description, such as new opacities and equations of state, and the employment of a new convection model more physically sound than the mixing-length theory. In a still more recent study, Hansen & Phinney (1998a) presented evolutionary calculations for these objects as well. However, the evolutionary sequences for their more massive models do not converge to the Hamada & Salpeter (1961) predictions for zero-temperature, pure-helium configurations, thus resulting in models with underestimated surface gravities. This can be seen from fig. 16 of Hansen & Phinney (1998a). Note that the surface gravity for their more massive models with a hydrogen envelope of $M_{\rm H}/{\rm M}_{\odot} = 10^{-6}$ is substantially lower than the Hamada–Salpeter values. Such a discrepancy cannot be attributed to the hydrogen layer, since a thin hydrogen envelope introduces a very small correction to the stellar radius of zero-temperature, pure helium models (see Benvenuto & Althaus 1998).

By contrast, the study of the evolution of carbon–oxygen white dwarfs has captured the interest of numerous investigators, such as Lamb & Van Horn (1975), Iben & Tutukov (1984), Koester & Schönberner (1986), D'Antona & Mazzitelli (1989), Tassoul, Fontaine & Winget (1990), Wood (1992), Benvenuto & Althaus (1997) and Althaus & Benvenuto (1998). In particular, Iben & Tutukov (1984) were the first in computing evolutionary models of white dwarfs with hydrogen burning, showing that hydrogen burning in cooling white dwarfs could be an important energy source.

With the calculations that we present here, we amply extend those presented in Althaus & Benvenuto (1997a) and Benvenuto & Althaus (1998), in which the effects of convection, neutrino losses and different hydrogen envelopes on the structure and evolution of helium white dwarfs were carefully analysed [we should mention that the results shown in Benvenuto & Althaus (1998) correspond to a metallicity of $Z \approx 0$ and not to $Z = 0.001$, as stated in that work]. Furthermore, we extend our calculations to the case of more massive carbon–oxygen white dwarfs. Our grid for carbon–oxygen models is likewise very detailed, which may be of relevance in the study of, for instance, the general problem of determining the theoretical white dwarf luminosity function and the assessment of the age of the Galactic disc. This subject has been recently addressed by Leggett, Ruiz & Bergeron (1998), who have greatly improved the determination of the observed luminosity function for cool white dwarfs. In this regard, we shall derive theoretical luminosity functions from our cooling sequences in order to compare with the Leggett et al. observational data.

The results presented here constitute a very detailed and updated set which will be suitable, for instance, for the interpretation of recent and forthcoming observational data on low-mass white dwarfs in close binary systems. Finally, we apply our evolutionary models with helium cores to derive stellar masses of a sample of low-mass white dwarfs.

2 COMPUTATIONAL DETAILS

The evolutionary sequences have been obtained with the same evolutionary code and input physics as we employed in our previous works on white dwarf evolution, and we refer the reader to Althaus & Benvenuto (1997a, 1998) and Benvenuto & Althaus (1998), as well as to the references cited therein, for details. In what follows we restrict ourselves to a few brief comments.

The code has been written following the method presented by Kippenhahn, Weigert & Hofmeister (1967) for calculating stellar evolution. In particular, to specify the surface boundary conditions we perform three envelope integrations (at constant luminosity) from photospheric starting values inward to a fitting mass fraction $M_1/M \approx 10^{-16}$, where M_1 corresponds to the first Henyey mass shell and M is the total mass of the white dwarf model. In our code the value of M_1 is automatically changed over the evolution so as to keep the thickness of the envelope as small as possible. This provides an accurate description of the outer layers of our white dwarf models. The interior integration is treated according to the standard Henyey technique as described by Kippenhahn et al. (1967).

The constitutive physics of our code is as detailed and updated as possible. Briefly, for the low-density regime, we consider the equation of state of Saumon, Chabrier & Van Horn (1995) for hydrogen and helium plasmas. The treatment for the high-density, completely ionized regime appropriate for the white dwarf interior is based on our own equation of state. This includes ionic and photon contributions, Coulomb interactions, partially degenerate electrons, quantum corrections for the ions and electron exchange and Thomas–Fermi contributions at finite temperature [see Althaus & Benvenuto (1997a) for details]. Radiative opacitites for the high-temperature regime ($T \geq 6000$ K) are those of OPAL (Iglesias & Rogers 1993), whilst for lower temperatures we use the Alexander & Ferguson (1994) molecular opacities [or the Cox & Stewart (1970) tabulation for pure helium composition]. Two extreme values for metallicity have been considered in the envelope: $Z = 0$ and 0.001. We should mention that, owing to the lack of reliable low-temperature ($T < 6000$ K) opacities for helium composition, our low-luminosity models with helium atmospheres should be regarded with caution, particularly their ages. Conductive opacities for the liquid and crystalline phases and the various mechanisms of neutrino emission relevant to white dwarf interiors are taken from the works of Itoh and collaborators [see Althaus & Benvenuto (1997a) for details]. We also include in our code the complete network of thermonuclear reaction rates for hydrogen burning corresponding to the proton–proton chain and the CNO bi-cycle. Nuclear reaction rates are taken from Caughlan & Fowler (1988) and β-decay rates from Wagoner (1969). Electron screening is from Wallace, Woosley & Weaver (1982). We use an implicit method of integration to compute the change of the following chemical species: ^{1}H, ^{2}H, ^{3}He, ^{4}He, ^{7}Li, ^{7}Be, ^{8}B, ^{12}C, ^{13}C, ^{13}N, ^{14}N, ^{15}N, ^{15}O, ^{16}O, ^{17}O and ^{17}F.

Another important feature of our evolutionary sequences is that the energy transport by convection is described by the full-spectrum turbulence theory [see Canuto & Mazzitelli (1991, 1992) and references cited therein for details], which represents a great improvement compared with the mixing-length theory of convection used thus far in most white dwarf studies. As a matter of fact, the Canuto & Mazzitelli theory, which has successfully passed a wide variety of laboratory and astrophysical tests (Canuto 1996), takes into account the whole spectrum of turbulent eddies necessary to compute the convective flux accurately in the almost inviscid

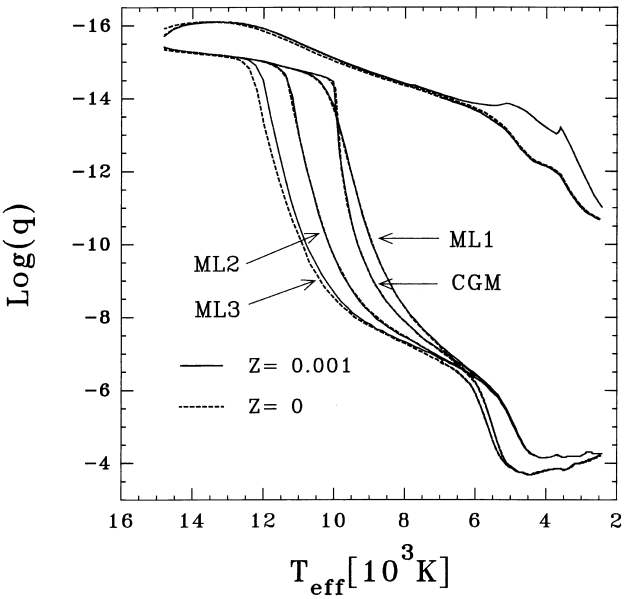

Figure 1. The location of the top and the base of the convection zone expressed in terms of the outer mass fraction q ($q = 1 - M_r/M$) versus $T_{\rm eff}$ for a 0.3-$M_\odot$ white dwarf model with a hydrogen envelope of $M_H/M = 10^{-3}$ according to different theories of convection and metallicities. It is clear that the mixing temperature for models with thin hydrogen envelopes will be dependent upon the assumed theory of convection. At low $T_{\rm eff}$ values, the depth reached by the base of the convection zone is independent of the treatment of convection. Note also the deeper final extent reached by convection in the case of metallicity $Z = 0$.

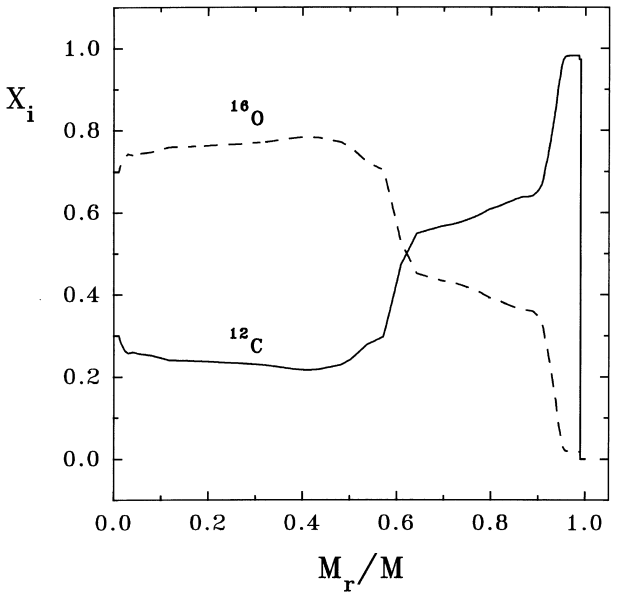

Figure 2. Chemical profile for our carbon–oxygen core models versus the fractional mass. Solid lines correspond to carbon and dashed lines to oxygen.

stellar interiors. For the set of sequences presented in this paper we have considered the recent improvement to this convection theory introduced by Canuto, Goldman & Mazzitelli (1996), which has been shown to provide a good agreement with recent observational data on pulsating white dwarfs (Althaus & Benvenuto 1997b). The model presented by Canuto et al. improves upon its predecessor (where the rate of input energy is given by the linear growth rate) in the fact that the growth rate is computed as a function of the turbulence itself, thus ensuring a self-consistent treatment. At intermediate and low convective efficiency, this feature leads to larger convective fluxes as compared with the Canuto & Mazzitelli (1992) model. It is worthwhile mentioning that the mass–radius relation and ages corresponding to our white dwarf models are practically insensitive to the convection theory employed. In contrast, the size of the outer convection zone in an intermediate effective temperature ($T_{\rm eff}$), evolving white dwarf is strongly dependent upon the assumed treatment of convection. Hence a trustworthy model of stellar convection must be employed to get reliable $T_{\rm eff}$ values at which thin hydrogen envelopes mix with the underlying helium (see Benvenuto & Althaus 1998). In this context, our calculations represent an improvement over previous white dwarf studies based on the mixing-length theory of convection. To clarify this point better, we show in Fig. 1 the behaviour of the evolving outer convection zone in terms of $T_{\rm eff}$ for our 0.3-$M_\odot$ model with a thick hydrogen envelope. In addition to Canuto et al.'s results, we include in the figure the predictions given by the ML1, ML2 and ML3 versions of the mixing-length theory amply used in white dwarf studies (see e.g. Tassoul et al. 1990). It is clear that the mixing $T_{\rm eff}$ for models with thin hydrogen envelopes depends upon the convection theory. Another observation that we can make from this figure is that the base of the convection zone (for the case $Z = 0$) ultimately reaches a final extent at an outer mass fraction $(1 - M_r/M)$ of 2×10^{-4} ($6 \times 10^{-5}\,M_\odot$), irrespective of the treatment of convection. This result is in good agreement with the predictions of Hansen & Phinney (1998a) for the same model. Note also the larger final extent of the convection zone for lower metallicity, which, as we shall see, gives rise to considerable differences in the evolutionary times at low luminosities.

Our white dwarf initial models of different masses and hydrogen envelopes have been obtained following the artificial evolutionary procedure described by Benvenuto & Althaus (1998). The carbon–oxygen core models all have the same core chemical composition profile as shown in Fig. 2. This chemical profile was calculated by D'Antona & Mazzitelli (1989) for the progenitor evolution of a 0.55-$M_\odot$ white dwarf. We adopt this profile for all of our models, in spite of the changes that are expected to occur for more massive models as a result of differences in the evolution in progenitor objects. We would need, in order to improve this assumption, detailed calculations of the pre-white dwarf evolution of these objects. To our knowledge, such calculations are not available. Because of the fact that the mass of the hydrogen envelope in white dwarfs is poorly constrained by theoretical calculations of the pre-evolution of these objects, particularly in the case of helium white dwarfs where the uncertainties regarding the mass-exchange episodes are more severe, we decide to treat the mass of the hydrogen envelope as essentially a free parameter. It is worthwhile mentioning that our evolving low-mass white dwarf models should be considered as evolutionary stages that can be asymptotically reached by helium white dwarfs resulting from close binary evolution. In this study we have not computed such binary evolution, and we refer the reader to Iben & Livio (1993) for a review. Needless to say, the starter model choice affects the *initial* evolution of all of our models, particularly the age [see Althaus & Benvenuto (1997a) for details].

In closing, we have included in our calculations the release of latent heat during crystallization [see Benvenuto & Althaus (1997) for details] and convective mixing.

3 THE GRIDS OF WHITE DWARF MODELS

In this section we comment on the most important features of the

grids. We have computed evolutionary sequences with masses ranging from $M = 0.1$ to $1.2\,M_\odot$ and metallicity $Z = 0.001$ and 0. For models with $M < 0.5\,M_\odot$ we assume a pure helium core and for models with $M > 0.45\,M_\odot$ we assume a carbon–oxygen core with the chemical profile of Fig. 2. We also vary the mass of the hydrogen envelope M_H within the range $10^{-12} \leq M_H/M \leq 4 \times 10^{-3}$ and the mass of the helium layer M_{He} (in the case of carbon–oxygen white dwarfs) is taken to be $M_{He}/M = 10^{-2}$. In Tables 1 and 2 we summarize the main characteristics of all of our available evolutionary sequences. As stated earlier, models have been calculated in the framework of the Canuto et al. (1996) theory of convection. We have used OPAL opacity calculations supplemented with the Alexander & Ferguson (1994) molecular opacities [or with the Cox & Stewart (1970) tabulation for helium composition] for low temperatures. In Tables 1 and 2 we also give the $T_{\rm eff}$ values at which each evolutionary sequence starts. In this regard, we emphasize once again that model ages corresponding to the *first* stages of evolution are meaningless because they are strongly affected by the procedure we use to generate the initial models. At advanced ages, however, this is no longer relevant and age values are meaningful. The sequences have been evolved down to a stellar luminosity $\log(L/L_\odot) = -5$.

We begin by examining the time evolution of our models. From the point of view of an age determination of the disc of our Galaxy from the observed space density of white dwarfs, the evolutionary times of white dwarfs as a function of mass obviously represent an important issue [see Wood (1992) and references cited therein]. In this regard, we feel it to be valuable to compare our cooling curves against those published by other authors. We elect those computed by Wood (1995) for models with pure oxygen cores on the basis of OPAL radiative opacities. To this end, we have computed additional sequences for models with oxygen cores and with the same outer layer chemical stratification and metallicity as considered by Wood. The comparison is shown in Fig. 3 for 0.5- and 0.7-$M_\odot$ models. Note the good agreement between the two sets of calculations. At very low luminosities and especially for more massive models than those considered in Fig. 3, some divergency appears as a result in part of the different set of low-temperature radiative opacities employed.

As we mentioned, white dwarf evolutionary times represent a

Table 1. Available white dwarf evolutionary sequences with a hydrogen envelope.

Sequence	$T_{\rm eff}^{\rm i}$	Sequence	$T_{\rm eff}^{\rm i}$	Sequence	$T_{\rm eff}^{\rm i}$	Sequence	$T_{\rm eff}^{\rm i}$
He151e3.z3	8.12	He151e4.z3	8.97	He151e6.z3	9.53	He151e8.z3	9.97
He152e3.z3	7.80	He152e4.z3	8.80	He154e3.z3	7.61	He154e4.z3	8.62
He201e3.z3	11.87	He201e4.z3	13.96	He201e6.z3	14.75	He201e8.z3	14.97
He202e3.z3	11.93	He202e4.z3	12.71	He204e3.z3	11.38	He204e4.z3	12.71
He251e3.z3	17.28	He251e4.z3	19.04	He251e6.z3	20.24	He251e8.z3	21.35
He252e3.z3	16.41	He252e4.z3	18.77	He254e4.z3	18.32	He301e3.z3	22.14
He301e4.z3	23.92	He301e6.z3	25.76	He301e8.z3	26.15	He302e3.z3	21.73
He302e4.z3	23.43	He304e4.z3	22.64	He351e3.z3	23.90	He351e4.z3	24.65
He351e6.z3	25.51	He351e8.z3	25.82	He352e4.z3	24.00	He354e4.z3	24.02
He361e3.z3	26.14	He371e3.z3	26.57	He381e3.z3	27.66	He391e3.z3	28.78
He401e3.z3	22.50	He401e4.z3	27.31	He401e6.z3	28.72	He401e8.z3	30.55
He402e4.z3	26.61	He404e4.z3	25.47	He411e3.z3	30.52	He428e4.z3	31.10
He429e4.z3	31.28	He439e4.z3	32.00	He448e4.z3	32.84	He451e4.z3	31.11
He451e6.z3	29.30	He451e8.z3	30.67	He452e4.z3	29.77	He454e4.z3	27.96
He458e4.z3	34.20	He468e4.z3	35.60	He501e4.z3	36.62	He501e6.z3	39.18
He501e8.z3	38.22	He502e4.z3	37.07	He504e4.z3	35.85		
OC501e4.z3	57.91	OC501e6.z3	60.78	OC501e8.z3	61.90	OC50e10.z3	61.31
OC50e12.z3	61.42	OC601e4.z3	61.07	OC601e6.z3	70.69	OC601e8.z3	72.04
OC60e10.z3	74.69	OC60e12.z3	74.81	OC701e4.z3	73.47	OC701e6.z3	78.56
OC701e8.z3	87.23	OC70e10.z3	87.94	OC70e12.z3	88.07	OC801e4.z3	91.60
OC801e6.z3	99.48	OC801e8.z3	101.14	OC80e10.z3	108.68	OC80e12.z3	108.83
OC901e6.z3	121.03	OC901e8.z3	122.79	OC90e10.z3	120.61	OC90e12.z3	122.81
OC101e6.z3	134.59	OC101e8.z3	136.49	OC10e10.z3	136.19	OC10e12.z3	136.37
OC111e6.z3	198.47	OC111e8.z3	196.97	OC11e10.z3	195.85	OC11e12.z3	194.00
He154e3.z0	7.70	He201e4.z0	14.05	He204e3.z0	11.37	He251e3.z0	17.01
He251e4.z0	18.93	He252e3.z0	16.38	He301e3.z0	20.55	He301e4.z0	23.63
He302e3.z0	21.70	He351e3.z0	23.50	He351e4.z0	24.83	He401e3.z0	22.69
He401e4.z0	27.14	He454e4.z0	29.49				
OC451e4.z0	43.28	OC471e4.z0	45.29	OC501e4.z0	58.49	OC521e4.z0	60.08
OC541e4.z0	53.71	OC561e4.z0	49.94	OC581e4.z0	49.65	OC601e4.z0	58.86
OC621e4.z0	57.49	OC641e4.z0	61.79	OC661e4.z0	62.33	OC681e4.z0	67.93
OC701e4.z0	77.50	OC721e4.z0	77.90	OC741e4.z0	79.33	OC761e4.z0	83.65
OC781e4.z0	85.30	OC801e4.z0	81.06	OC821e4.z0	81.79	OC841e4.z0	89.26
OC901e4.z0	106.71	OC101e4.z0	106.95	OC111e4.z0	95.00	OC121e6.z0	96.65
OC121e8.z0	97.27						

Note. This table shows available evolutionary sequences for white dwarf models with a hydrogen envelope. We use an abbreviated notation to indicate the core composition, the stellar mass in tenths of solar mass units, the mass fraction of the hydrogen envelope and the envelope metallicity. For instance, He252e3.z0 stands for an evolutionary sequence of $0.25\,M_\odot$ models with a helium core composition, a hydrogen envelope of $M_H/M = 2 \times 10^{-3}$ and an envelope metallicity of $Z = 0$. OC means a oxygen–carbon core composition. (Note that OC sequences for models more massive than $1\,M_\odot$ are indicated with the same notation.) We also provide a column ($T_{\rm eff}^{i}$) for the effective temperature (in thousand of degrees K) at which each sequence starts.

Table 2. Available white dwarf evolutionary sequences without a hydrogen envelope.

Sequence	$T_{\rm eff}^i$	Sequence	$T_{\rm eff}^i$	Sequence	$T_{\rm eff}^i$	Sequence	$T_{\rm eff}^i$
He0990.z3	6.62	He1039.z3	7.00	He1091.z3	7.45	He1146.z3	7.93
He1203.z3	8.45	He1263.z3	9.02	He1326.z3	9.62	He1393.z3	10.26
He1462.z3	10.99	He1500.z3	11.59	He1575.z3	12.17	He1654.z3	12.90
He1736.z3	13.51	He1823.z3	14.08	He1914.z3	14.82	He2010.z3	15.85
He2110.z3	17.26	He2216.z3	18.27	He2327.z3	20.01	He2443.z3	21.42
He2565.z3	22.83	He2693.z3	24.61	He2829.z3	25.29	He2970.z3	26.70
He3118.z3	26.44	He3274.z3	26.77	He3438.z3	27.90	He3610.z3	28.07
He3790.z3	30.09	He3979.z3	29.63	He4179.z3	30.60	He4388.z3	32.49
He4607.z3	34.63	He4837.z3	37.30	He5079.z3	37.69		
OC5000.z3	57.61	OC5200.z3	47.60	OC5400.z3	51.96	OC5600.z3	54.21
OC5800.z3	59.70	OC6000.z3	78.72	OC7000.z3	78.59	OC8000.z3	93.85
OC9000.z3	94.82	OC1000.z3	101.57	OC1100.z3	107.97	OC1200.z3	100.01

Note. This table shows available evolutionary sequences for white dwarf models without a hydrogen envelope. We use an abbreviated notation to indicate the core composition, the stellar mass in tenths of solar mass units and the envelope metallicity. For instance, He3118.z3 stands for an evolutionary sequence of 0.3118-$M_\odot$ models with a helium core composition and an envelope metallicity of $Z = 0.001$. OC means oxygen–carbon core composition. (Note that OC sequences for models more massive than 1 $M_\odot$ are indicated with the same notation.) We also provide a column ($T_{\rm eff}^i$) for the effective temperature (in thousands of degrees K) at which each sequence starts.

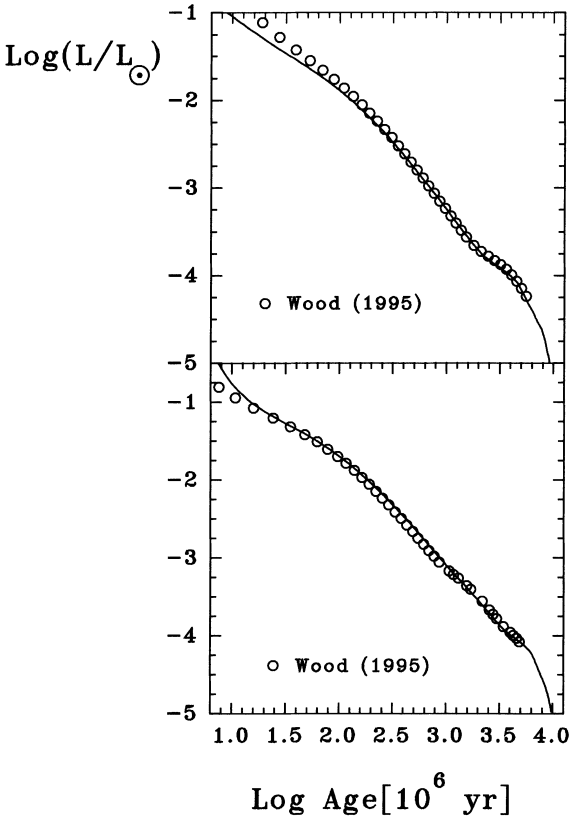

Figure 3. Age–surface luminosity relation for 0.5- (upper panel) and 0.7- (lower panel) $M_\odot$ white dwarf models with pure oxygen cores and a hydrogen envelope mass of $M_{\rm H}/M = 10^{-4}$. We compare our results (solid lines) with those given by the Wood (1995) models (open circles) having the same stellar mass and chemical stratification as ours. The calculations are for a metallicity of $Z = 0$. At high luminosities, the discrepancy between the two sets of calculations is due to the different procedure employed to generate the initial models.

powerful tool for constraining the age of the disc of our Galaxy. Indeed, the existence of an abrupt fall-off in the observed white dwarf luminosity function [see Liebert, Dahn & Monet (1988) and earlier references cited therein] has been interpreted in terms of a finite age of the disc of the Galaxy (D'Antona & Mazzitelli 1978). By fitting the observations with theoretical white dwarf luminosity functions, this interpretation was quantitatively explored by numerous investigators such as Winget et al. (1987), Iben & Laughlin (1989) and Wood (1992). Recently, Leggett et al. (1998) have substantially improved the determination of the observed luminosity function for cool white dwarfs. To compare with observations, we have constructed integrated luminosity functions from our evolutionary sequences. To this end, we follow the treatment presented in Iben & Laughlin (1989). Specifically, the space density of white dwarfs per unit of ℓ, $\ell \equiv \log(L/{\rm L}_\odot)$, is calculated from

$$\frac{{\rm d}n}{{\rm d}\ell} = -\psi_0 \int_{m_{\rm i}}^{m_{\rm s}} \phi(m) \left(\frac{\partial t_{\rm cool}}{\partial \ell}\right)_M {\rm d}m. \quad (1)$$

Here, $\phi(m)$ is the Salpeter initial mass function of white dwarf progenitors with stellar mass m (which predicts that the created stellar distribution is proportional to $1/m^{2.35}$) and $t_{\rm cool}$ is the white dwarf cooling time at a given ℓ, which is a function of the white dwarf mass M. $m_{\rm i}$ and $m_{\rm s}$ denote respectively the minimum and the maximum masses of the main-sequence stars which contribute to the white dwarf space density at ℓ. We take $m_s \approx 8\,{\rm M}_\odot$ (Wood 1992) and m_i is obtained by solving the equation $t_{\rm MS}(m) + t_{\rm cool}(\ell, M) = t_{\rm d}$, where $t_{\rm d}$ is the assumed disc age. The pre-white dwarf evolutionary times $t_{\rm MS}(m)$ are those of Iben & Laughlin (1989). As far as the initial(m)–final(M) mass relation is concerned, we use an exponential model: $M = 0.40{\rm e}^{0.125m}$ (Wood 1992). In deriving equation (1), the star formation rate ψ_0 has been assumed to be constant. Finally, for each of the selected luminosity values, we calculate $\partial t_{\rm cool}/\partial \ell$ at a given M by using linear interpolation between the $\partial t_{\rm cool}/\partial \ell$ values of the sequences that bracket M. The resulting luminosity functions for assumed disc ages of 6–10 Gyr are shown in Fig. 4 (in Fig. 4, the luminosity functions have been converted into intervals of bolometric magnitude $M_{\rm bol}$). It is worth mentioning that all of our theoretical curves have been normalized to the observed space density of 0.003 39 white dwarfs per cubic parsec (Leggett et al. 1998). The best fit to the

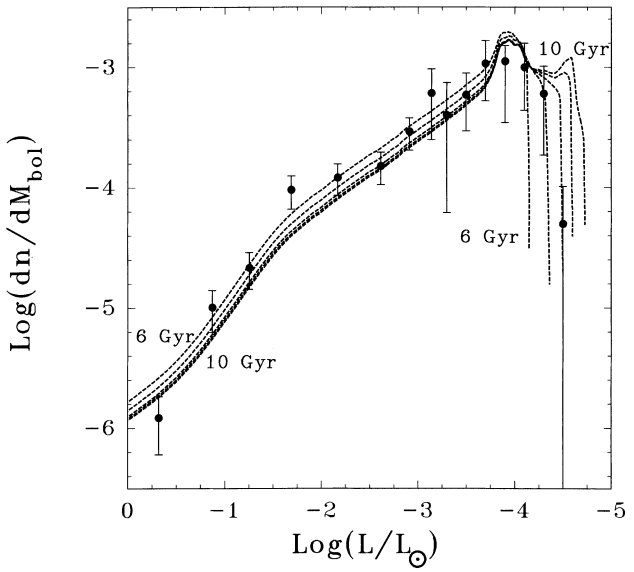

Figure 4. Theoretical white dwarf luminosity functions (dashed lines) corresponding to our carbon–oxygen core, white dwarf models with a hydrogen envelope mass of $M_H/M = 10^{-4}$ and metallicity $Z = 0$. The curves, which correspond to assumed disc ages of 6–10 Gyr (at intervals of 1 Gyr), are compared with the observational data of Leggett et al. (1998), and they have been normalized to the observed white dwarf space density of 0.003 39 stars per cubic parsec. Note that the best fit to the dimmest white dwarfs observed corresponds to a disc age of approximately 8 Gyr.

coolest white dwarfs observed is obtained for assumed disc ages of ≈8 Gyr, which is in agreement with the ages quoted by Leggett et al. on the basis of the Wood (1995) cooling sequences.

It is worthy of comment that the age of helium white dwarf models depends on the mass of the hydrogen envelope. This is particularly true for models with very thick hydrogen envelopes, for which hydrogen burning contributes substantially to the total luminosity, thus leading to a delay in cooling even down to very low $T_{\rm eff}$. Unfortunately, the maximum mass of the hydrogen envelope resulting from binary evolution is still an open question. Evidence favouring 'thin' envelopes was presented by Iben & Tutukov (1986) from self-consistent binary evolutionary calculations. Indeed, these authors found that the hydrogen envelope remaining at the top of their 0.3-$M_\odot$ remnant after shell flash episodes is too small ($M_H \approx 1.4 \times 10^{-4}\,M_\odot$) to sustain any further nuclear burning. Needless to say, a larger hydrogen remnant would lead to longer evolutionary times. In the context of age determinations of millisecond pulsars with helium white dwarf companions, this fact is a clearly important one to be taken into account. To place this assertion on a more quantitative basis, we consider the pulsar PSR J1012+5307. The surface gravity and $T_{\rm eff}$ for its low-mass helium white dwarf companion have been determined to be $\log g = 6.75 \pm 0.07$ and $T_{\rm eff} = 8550 \pm 25$ K (van Kerkwijk et al. 1996). At $T_{\rm eff} \approx 8500$ K, we find that our 0.21-$M_\odot$ helium white dwarf model with $M_H/M = 2 \times 10^{-3}$ has $\log g = 6.82$ and age 0.44 Gyr, in good agreement with the Hansen & Phinney (1998b) predictions. The same fit to the $T_{\rm eff}$ and gravity values would be achieved with a 0.213-$M_\odot$ model with $M_H/M \approx 6 \times 10^{-3}$. However, in this case hydrogen burning supplies 70 per cent of the surface luminosity and the model age becomes as high as 0.9 Gyr.

Our main motivation for the publication of a detailed set of low-mass white dwarf models like the one presented here is, apart from the fact that little attention has been paid in the past to the study of this kind of object, that both finite-temperature effects and hydrogen envelopes substantially modify the surface gravity values of zero-temperature, helium-core-degenerate configurations. These features may turn out to be very important for the interpretation of recent and future observational data on low-mass white dwarfs. We think that the detailed low-mass models that we have computed here by employing the full scheme of stellar evolution theory may help such an endeavour.

In the context of the foregoing paragraph, we show in Fig. 5 the surface gravity g (in cgs units) in terms of $T_{\rm eff}$ for some selected models. The effects of finite temperature are clearly noticeable, particularly for less massive models. As is well known, at a given $T_{\rm eff}$ more massive models are characterized by smaller radii. As $T_{\rm eff}$ decreases the model radius (gravity) gradually becomes smaller (larger), ultimately reaching an almost constant value as expected for a strongly degenerate configuration, in which the mechanical structure is determined mainly by degenerate electron pressure. As a result, stellar parameters asymptotically reach constant values corresponding to zero-temperature configurations. Note also the changes in the g-values brought about by rather thick hydrogen envelopes. Another observation we can make from this figure is that, at low $T_{\rm eff}$, convective mixing between hydrogen and helium layers increases the g-values of models with thin hydrogen envelopes. In fact, convective mixing changes the outer layer composition from a hydrogen-dominated to a helium-dominated one, thus giving rise to denser outer layers. From then on, their subsequent evolution resembles that of a white dwarf model without a hydrogen envelope, as can be noted from Fig. 5 (see also Fig. 6), particularly for less massive models.

To clarify better the role played by hydrogen envelopes in the g-values of low-mass models, we show in Fig. 6 the reduction in the g-values of pure helium configurations resulting from adding hydrogen envelopes of different thickness. More precisely, we plot

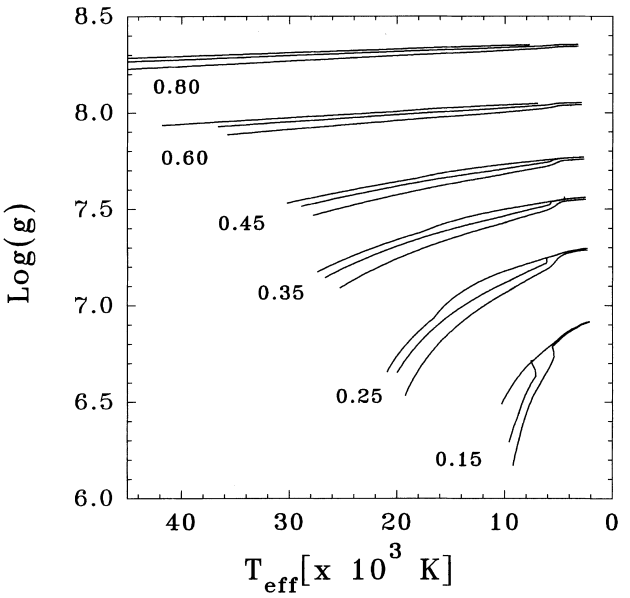

Figure 5. Surface gravities versus $T_{\rm eff}$ for selected white dwarf models with $M/M_\odot$ = 0.15, 0.25, 0.35, 0.45, 0.60 and 0.80 and different hydrogen envelopes. For each stellar mass and from top to bottom the curves correspond to sequences having hydrogen envelopes with fractional masses of $M_H/M = 0$ (no hydrogen envelope), 10^{-6} and 10^{-4}, respectively. Note that, in the case of less massive models, hydrogen envelopes appreciably reduce the surface gravity values of pure helium models.

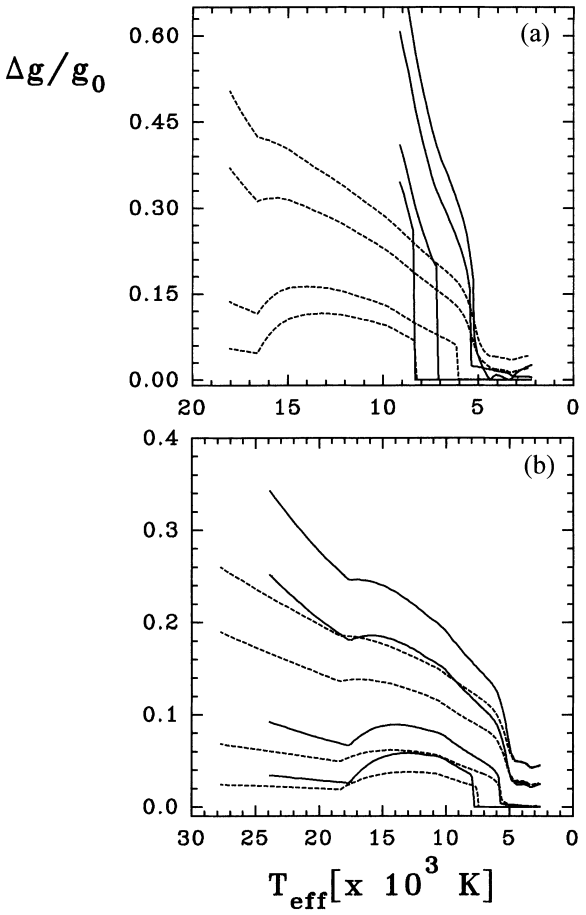

Figure 6. (a) Ratio of the difference in g-values between low-mass white dwarf models without (g_0) and with hydrogen envelopes to g_0, versus $T_{\rm eff}$ for models with $M/\,{\rm M}_\odot$ = 0.15 (solid lines) and 0.25 (dashed lines). For each stellar mass and from top to bottom the curves correspond to sequences with hydrogen envelopes of fractional mass $M_{\rm H}/M = 4\times10^{-4}$, 10^{-4}, 10^{-6} and 10^{-8}, respectively. (b) As (a) but for models with $M/\,{\rm M}_\odot = 0.35$ (solid lines) and 0.45 (dashed lines). Note that thick hydrogen envelopes appreciably reduce the g-values of pure helium models. Note also the effect of convective mixing at low $T_{\rm eff}$ on models with thin hydrogen envelopes.

in terms of $T_{\rm eff}$ the quantity $\Delta g/g_0 \equiv (g_0 - g_{\rm H})/g_0$ for various stellar masses and hydrogen envelopes (g_0 and $g_{\rm H}$ stand for the surface gravity of a helium-core configuration of a given stellar mass without and with a hydrogen envelope, respectively). It is clear that thick hydrogen envelopes appreciably reduce the g-values of pure helium models. At the low $T_{\rm eff}$ of 15 000 K, for instance, the g-values of the 0.35- and 0.25-$\,{\rm M}_\odot$ pure helium models are reduced, respectively, by 20 and 30 per cent if a hydrogen envelope of $M_{\rm H}/M = 10^{-4}$ is added. Such values increase considerably at higher $T_{\rm eff}$. At $T_{\rm eff}\approx$ 17 000 K, there is a change in the slope of the curves stemming from the decrease in the radiative opacity values after helium recombination. This causes pure helium models to become denser and hence to have larger g-values.

Non-negligible differences in the structure and cooling of white dwarfs may also arise from the employment of different metallicities in the envelope, particularly at low luminosities where the central temperature of the models becomes strongly tied to the details of the outer layer chemical stratification (see Tassoul et al. 1990). This expectation is borne out by Fig. 7, in which we compare the cooling times of helium white dwarf models for two extreme metallicities assumed in the envelope. When convection reaches the

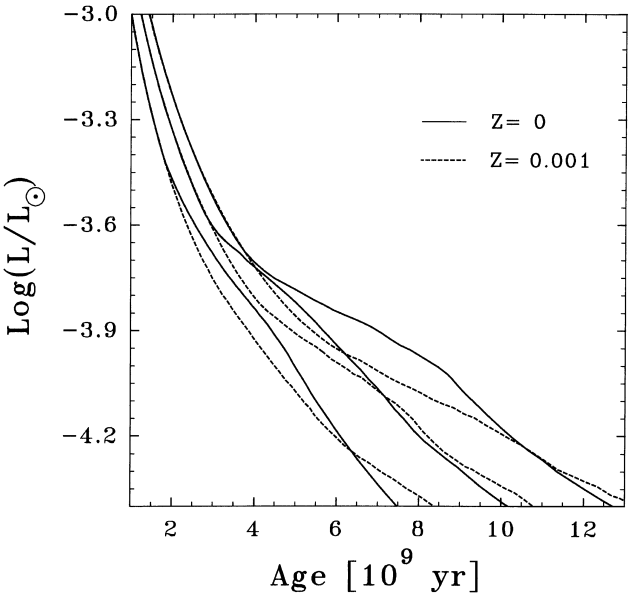

Figure 7. Surface luminosity versus age relation for (from top to bottom) 0.40-, 0.30- and 0.2-$\,{\rm M}_\odot$ helium white dwarf models with $M_{\rm H}/M = 10^{-4}$ and for metallicities $Z = 0$ (solid lines) and $Z = 0.001$ (dashed lines). Note that, at high luminosities, cooling is not affected by the assumed metallicity in the envelope.

domain of degeneracy, the central temperature drops substantially and the star has initially an excess of internal energy to be radiated, thus giving rise to a lengthening of the evolutionary times during that stage of evolution. Because models with lower metallicities are characterized by deeper convection zones (see Fig. 1), this effect occurs at higher luminosities in such models and this explains their greater ages as compared with high-metallicity models. Eventually, at very low luminosities, more transparent models evolve more rapidly, as expected. We have also analysed the effect of metallicity on surface gravity for helium models (see Fig. 8), and we have found that surface gravity is almost insensitive to a specific choice of metallicity in the envelope.

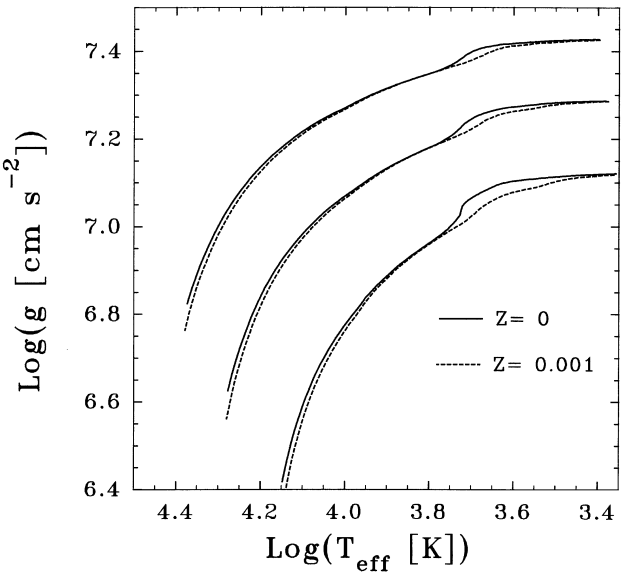

Figure 8. Surface gravity versus $T_{\rm eff}$ for (from top to bottom) 0.30-, 0.25- and 0.20-$\,{\rm M}_\odot$ helium white dwarf models with $M_{\rm H}/M = 10^{-4}$ and for metallicities $Z = 0$ (solid lines) and $Z = 0.001$ (dashed lines).

Table 3. Masses for low-mass white dwarfs.

White Dwarf	Source	$T_{\rm eff}$ (K)	log g	$M/M_{\odot}(1)$	$M/M_{\odot}(2)$	$M/M_{\odot}(3)$
$0316+345$	BSL	14880	7.61	0.40	0.414	0.452
$0339+523$	BSL	13350	7.47	0.34	0.354	0.395
$0710+741$	BSL	18930	7.45	0.35	0.377	0.418
$0957-666$	BRB	27047	7.285	0.335	0.371	0.417
$1022+050$	BRB	14481	7.483	0.351	0.364	0.405
$1101+364$	BSL	13610	7.38	0.31	0.325	0.369
$1241+010$	BSL	24010	7.22	0.31	0.342	0.390
$1317+453$	BSL	14000	7.43	0.33	0.343	0.385
$1353+409$	BSL	23580	7.54	0.40	0.427	0.470
$1614+136$	BSL	22430	7.34	0.33	0.361	0.409
$1713+332$	BSL	22030	7.40	0.35	0.376	0.420
$1824+040$	BRB	14795	7.608	0.394	0.411	0.451
$2032+188$	BSL	18540	7.48	0.36	0.385	0.425
$2331+290$	BSL	27830	7.50	0.39	0.431	0.479
$2337-760$	BRB	14295	7.507	0.354	0.372	0.410

Note. $T_{\rm eff}$, the surface gravity (g) and the stellar mass (1) of the objects are taken from Bergeron et al. (1992) (BSL) and Bragaglia et al. (1995) (BRB). The next column (2) gives the stellar mass according to our helium - core models without a hydrogen envelope, and the last column lists the stellar mass according to our helium - core models with a hydrogen envelope of $M_{\rm H}/M = 10^{-3}$.

Lastly, we have applied our evolutionary models with helium cores to derive stellar masses of some selected low-mass white dwarfs. To this end, we have picked out low surface gravity white dwarfs from the sample of white dwarfs analysed by Bergeron, Saffer & Liebert (1992) and Bragaglia, Renzini & Bergeron (1995), and we list the results in Table 3. The above-cited authors estimated the white dwarf masses from evolutionary models with pure carbon-core composition. However, using our evolutionary models with helium cores and no hydrogen envelope, we find the mass values to be appreciably underestimated, particularly at high temperatures. It is worth mentioning that the objects listed in Table 3 are white dwarfs that most likely have a hydrogen envelope. This being the case, the stellar mass should be estimated from evolutionary models with hydrogen envelopes. As shown in Table 3, there is an appreciable difference in the white dwarf mass when stellar masses are derived from models with thick hydrogen envelopes ($M_{\rm H}/M \approx 10^{-3}$).

In view of the preceding considerations, we conclude that detailed models of low-mass white dwarfs such as presented in this study should be carefully taken into account, should the mass of a white dwarf be measured by applying the surface gravity–$T_{\rm eff}$ relation. This is particularly true regarding the possibility of constraining the equation of state at neutron star densities as inferred from observations of low-mass white dwarf companions to millisecond pulsars, such as those studied by van Kerkwijk et al. (1996).

Complete tables containing the results of our calculations are available at the World Wide Web site http://www.fcaglp.unlp.edu.ar/~althaus/. Additional evolutionary sequences are obtained upon request to the authors at their e-mail addresses. Features such as surface luminosity, $T_{\rm eff}$, central density and temperature, surface gravity, stellar radius, age and hydrogen surface abundance are listed in the tables.

ACKNOWLEDGMENTS

We are indebted to F. D'Antona for sending us the starting model, and to F. Rogers for providing us with his radiative opacity data tables. We also thank T. Guillot and D. Saumon for their help in making available to us the low-density equation of state that we have employed here. We are also grateful to V. M. Canuto for providing us with the Canuto, Goldman & Mazzittelli model before publication. We also thank our anonymous referee, whose comments greatly improved the original version of this work.

REFERENCES

Alexander D. R., Ferguson J. W., 1994, ApJ, 437, 879
Althaus L. G., Benvenuto O. G., 1997a, ApJ, 477, 313
Althaus L. G., Benvenuto O. G., 1997b, MNRAS, 288, L35
Althaus L. G., Benvenuto O. G., 1998, MNRAS, 296, 206
Backer D. C., 1998, ApJ, 493, 873
Benvenuto O. G., Althaus L. G., 1997, MNRAS, 288, 1004
Benvenuto O. G., Althaus L. G., 1998, MNRAS, 293, 177
Bergeron P., Saffer R. A., Liebert J., 1992, ApJ, 394, 228 (BSL)
Bragaglia A., Renzini A., Bergeron P., 1995, ApJ, 443, 735 (BRB)
Burderi L., King A. R., Wynn G. A., 1996, MNRAS, 283, L63
Canuto V. M., 1996, ApJ, 467, 385
Canuto V. M., Mazzitelli I., 1991, ApJ, 370, 295
Canuto V. M., Mazzitelli I., 1992, ApJ, 389, 724
Canuto V. M., Goldman I., Mazzitelli I., 1996, ApJ, 473, 550
Caughlan G. R., Fowler W. A., 1988, At. Data Nucl. Data Tables, 40, 290
Cox A. N., Stewart J., 1970, ApJs, 19, 261
D'Antona F., Mazzitelli I., 1978, A&A, 66, 453
D'Antona F., Mazzitelli I., 1989, ApJ, 347, 934
Edmonds P. D., Grindlay J. E., Cool A., Cohn H., Lugger P., Bailyn C., 1998, ApJ, submitted
Hamada T., Salpeter E. E., 1961, ApJ, 134, 683
Hansen B. M. S., Phinney E. S., 1998a, MNRAS, 294, 557
Hansen B. M. S., Phinney E. S., 1998b, MNRAS, 294, 569
Iben I., Laughlin G., 1989, ApJ, 341, 312
Iben I., Jr, Livio M., 1993, PASP, 105, 1373
Iben I., Jr, Tutukov A. V., 1984, ApJ, 282, 615
Iben I., Jr, Tutukov A. V., 1986, ApJ, 311, 742
Iben I. Jr., Tutukov A. V., Yungelson L. R., 1997, ApJ, 475, 291
Iglesias C. A., Rogers F. J., 1993, ApJ, 412, 752
Kippenhahn R., Weigert A., Hofmeister E., 1967, in Alder B., Fernbach S., Rottenberg M., eds, Methods in Computational Physics, 7. Academic Press, New York, p. 129
Koester D., Schönberner D., 1986, A&A, 154, 125
Lamb D. Q., Van Horn H. M., 1975, ApJ, 200, 306
Landsman W., Aparicio J., Bergeron P., Di Stefano R., Stecher T. P., 1997, ApJ, 481, L93
Leggett S. K., Ruiz M. T., Bergeron P., 1998, ApJ, 497, 294

Liebert J., Dahn C. C., Monet D. G., 1988, ApJ, 332, 891
Lundgren S. C., Cordes J. M., Foster R. S., Wolszczan A., Camilo F., 1996, ApJ, 458, L33
Marsh T. R., 1995, MNRAS, 275, L1
Marsh T. R., Duck S. R., 1996, MNRAS, 278, 565
Marsh T. R., Dhillon V. S., Duck S. R., 1995, MNRAS, 275, 828
Moran C., Marsh T. R., Bragaglia A., 1997, MNRAS, 288, 538
Renzini A. et al., 1996, ApJ, 465, L23
Richer B. H. et al., 1995, ApJ, 451, L17
Saumon D., Chabrier G., Van Horn H. M., 1995, ApJs, 99, 713
Tassoul M., Fontaine G., Winget D. E., 1990, ApJs, 72, 335
van Kerkwijk M. H., Bergeron P., Kulkarni S. R., 1996, ApJ, 467, L89
Von Hippel T., Gilmore G., Jones D. H. P., 1995, MNRAS, 273, L39
Wagoner R. V., 1969, ApJs, 18, 247
Wallace R. K., Woosley S. E., Weaver T. A., 1982, ApJ, 258, 696
Winget D. E. et al., 1987, ApJ, 315, L77
Wood M. A., 1992, ApJ, 386, 539
Wood M. A., 1995, in Koester D., Werner K., eds, NATO ASI Series, Nineth European Workshop on White Dwarfs. Springer, Berlin, p. 41

This paper has been typeset from a TEX/LATEX file prepared by the author.